Heterosynaptic plasticity in biomembrane memristors controlled by pH

Haden Scott,[1] William T. McClintic, [2] Nick Moore,[3] Mikayla Maxwell,[3] Mustafa Farahat,[4] Dima Bolmatov,[5] Francisco Barrera,[3] John Katsaras,[1,6] C. Patrick Collier [2,7*]

[1]Labs and Soft Matter Group, Neutron Scattering Division, Oak Ridge National Laboratory, Oak Ridge, Tennessee 37831; [2]Bredesen Center for Interdisciplinary Research, University of Tennessee, Knoxville, Tennessee 37996; [3]Department of Biochemistry & Cellular and Molecular Biology, University of Tennessee, Knoxville, Tennessee 37996; [4]Department of Chemical and Biomolecular Engineering, University of Tennessee, Knoxville, Tennessee 37996; [5]; [6]Shull Wollan Center, Oak Ridge National Laboratory, Oak Ridge, Tennessee 37831; [7]Center for Nanophase Materials Sciences, Oak Ridge National Laboratory, Oak Ridge, Tennessee 37831

[7]Center for Nanophase Materials Sciences, Oak Ridge National Laboratory, Oak Ridge, Tennessee 37831

*To whom correspondence should be addressed: colliercp@ornl.gov

Abstract

In biology, heterosynaptic plasticity maintains homeostasis in synaptic inputs during associative learning and memory and can initiate long-term changes in synaptic strengths that nonspecifically modulate numerous synapse types. In bioinspired neuromorphic circuits, heterosynaptic plasticity may be used to extend the functionality of two-terminal, biomimetic memristors. In this paper, we explore how changes in the pH of the aqueous solutions that make up the two droplets in a droplet interface bilayer (DIB) modulate the memristive responses of a lipid bilayer membrane in the pH range 4.97 to 7.40. The current responses to voltage stimulation were noisy, and as a result, we did not find conclusive evidence for pH-dependent shifts in this range in the voltage thresholds (V^*) needed for alamethicin ion channel formation in the membrane. This was surprising considering that changes in the elastic curvature properties of phospholipid bilayers that result in increased ionic currents are known to occur at lower pH. We did however see a clear modulation in the *dynamics* of pore formation with pH in time-dependent, pulsed voltage experiments. At the same voltage, lowering pH resulted in higher steady-state currents, by shifting the equilibrium concentrations of peptide aggregate assemblies in the membrane to favor larger, more conductive pores. It also increased potentiation time constants for pore formation and enhanced short-term facilitation and depression of the switching characteristics of the device. These changes were due in part to shifts in the elastic curvature behavior of the lipid bilayer at lower pH. This increased ionic current through the pores and the partitioning of alamethicin into the nonpolar lipid tail region of the membrane upon neutralization of the charged carboxylate groups on each monomer, making the monomers more hydrophobic. Modulating these thresholds independently of alamethicin concentration and applied voltage enables the construction of neuromorphic circuitry with enhanced, complex functionality.

Impact Statement

We describe the use of pH as a modulatory "interneuron" that changes the voltage-dependent memristance of alamethicin ion channels in lipid bilayers by changing the structure and dynamical

properties of the bilayer itself. Having the ability to control the threshold levels for pore conduction independently from voltage or ion channel concentration enables additional levels of programmability in a neuromorphic system to realize a wider array of functionalities. In this report, we note that thresholds for the onset of conduction from membrane-bound ion channels can be lowered by reducing solution pH, resulting in higher currents through the channels, and enhanced short-term learning behavior in the form of paired-pulse facilitation (PPF) and paired-pulse depression (PPD). Tuning threshold values with environmental variables like pH provides additional training and learning algorithms that can be used to elicit complex functionality within spiking neural networks (SNNs).

Keywords: *membrane, neuromorphic, biomimetic, synaptic plasticity, interface*

Introduction

Synaptic plasticity refers to the ability of a synaptic connection between neurons to change its strength. Homosynaptic plasticity refers to synaptic connections that are input specific, meaning activity at a specific, neuron is responsible for the strength of the synaptic connections with that neuron. However, there are also examples of heterosynaptic plasticity, or synaptic plasticity involving much larger populations of synapses and neurons where specific synaptic connections are not directly targeted. In biology, heterosynaptic plasticity maintains homeostasis in synaptic inputs during associative learning and memory, and can initiate extended, long-lasting changes in synaptic strengths that are not specific to any one synapse but can indirectly modulate many synapses in an extended neural circuit. [1]

Heterosynaptic plasticity may extend the functionality of bioinspired neuromorphic circuits consisting of memristors and memcapacitors, by enabling additional parameters with which to modulate short-term and long-term synaptic plasticity in these circuits. Heterosynaptic plasticity involves “interneurons” that can modulate the communication efficiency of synapses in neural circuits without affecting any one synapse. [2] Interneurons in solid state devices can be gate electrodes in three-terminal synaptic transistors [3] or auxiliary structures that can apply electric and magnetic fields that modulate memristive properties locally between the presynaptic and postsynaptic electrodes in tunnel junctions. [4] In two-terminal soft-matter memristors based on lipid bilayer membranes and membrane-associated ion channels, interneurons could be developed to globally modulate the voltage-dependent conductance and capacitance of the bilayer. These would not necessarily require a physical third electrode, but instead could be based on environmental changes affecting many synapses, such as pH, ionic strength, and temperature. These external variables can change the structure and dynamical properties of ion channels, and of the bilayer in which they are embedded.

Changes in pH can be used to titrate the ionizable groups of charged lipid bilayers, such as phosphatidylserine (PS), which has three ionizable groups and is negatively charged at neutral pH. Phosphatidylcholine (PC), a frequently used component of lamellar lipid bilayers, is zwitterionic, and therefore net neutral without ionizable groups except at extreme values of pH. [5] Nevertheless, even relatively “modest” changes in pH can charge PC lipid bilayers with embedded ion channels similarly to those in charged PS lipid bilayers.

Previously, we reported on short-term synaptic plasticity in artificial synapses via the memristive behavior in alamethicin (alm)-doped diphytanoylphosphatidyl choline (DPhPC) lipid membranes. DPhPC is a synthetic PC lipid known for its chemical stability and low ion permeability in DIBs, a membrane platform which consist of two aqueous droplets in oil (hexadecane), each coated with a monolayer of lipids, that form a lipid bilayer between them. [6,7] For this study, we explored how changes in DIB pH modulate the memristive responses of the membrane. A reasonable expectation is that the largest observable effect would be a shift in the voltage threshold (V^*) needed to form conductive pores in the membrane. These thresholds are important components of memristive behavior in that they are partially responsible for the "pinched hysteresis" in current-voltage (I/V) plots and the hallmark of a memristive system. [cite Chua] Surprisingly, we were not able to definitively link changes in pH with shifts in V^* beyond simple, random noise. This does not necessarily mean that such a link does not exist. Even at the same pH, the V^* values we measured were stochastic, and any link with changes in pH may have been so weak that they were overwhelmed by the system's intrinsic noise. We did however find a clear link between the pH and the time dependent current responses to voltage pulses, which can also be used to detect and categorize memristive behavior. At low pH, we found increased current levels at the same V^*, pore conduction onset at lower V^* values, and enhanced short-term synaptic plasticity in the form of increased paired-pulse facilitation (PPF) and paired-pulse depression (PPD) of the switching conductance. These findings will help in enabling the construction of neuromorphic circuitry with enhanced, complex functionality.

Results

Figure 1 is an overview of the process used to look for shifts in V^* voltage threshold values with changes in pH. In Figure 1a, above a characteristic voltage threshold, V^*, alm monomers undergo a phase transition from a surface-associated (S) state, where their long axis of the channel forming peptide is parallel to the plane of the bilayer, to an inserted (I) state, where they can monomers in the membrane oligomerize into conductive pores. In this scenario, increases in ionic current for voltages greater than a voltage threshold ($V > V^*$) are the result of a higher *number* of conductive pores in the membrane rather than any intrinsic increases in pore conductance. [cite] Figure 1b shows a corresponding downward shift in V^* values to lower voltages at lower pH, at a scan rate of 10 mV/s. Faster scan rates (100, 250, and 500 mV/s) resulted in the well-known "pinched hysteresis" characteristics associated with memristive behavior in alm-DPhPC bilayer membranes. [7] These are due to the development of lag times between the formation of conductive pores in the membrane, governed by the voltage threshold at V^*, and voltage-dependent changes to the membrane area of the DIB because of electrowetting.

The inset to Figure 1c shows the growth of the positive lobe of a hysteresis loop generated by steady-state currents from alm pores in DPhPC lipid bilayers, as functions of voltage. The main graph shows the first current vs. voltage trajectory of the loop, which extends from zero volts to past the V^* voltage threshold for ion channel conduction. This threshold is defined as 10x the background conductance, which is 8 $\mu S/cm^2$ (plotted as the black dashed line in the figure). [cite] V^* is defined as the voltage where the current from the alm-DPhPC bilayer first overtakes this threshold current (blue dashed circle) – the majority of the threshold crossings occurred later, and at lower voltages. Figure 1D shows probability density distributions as histograms of V^* at the

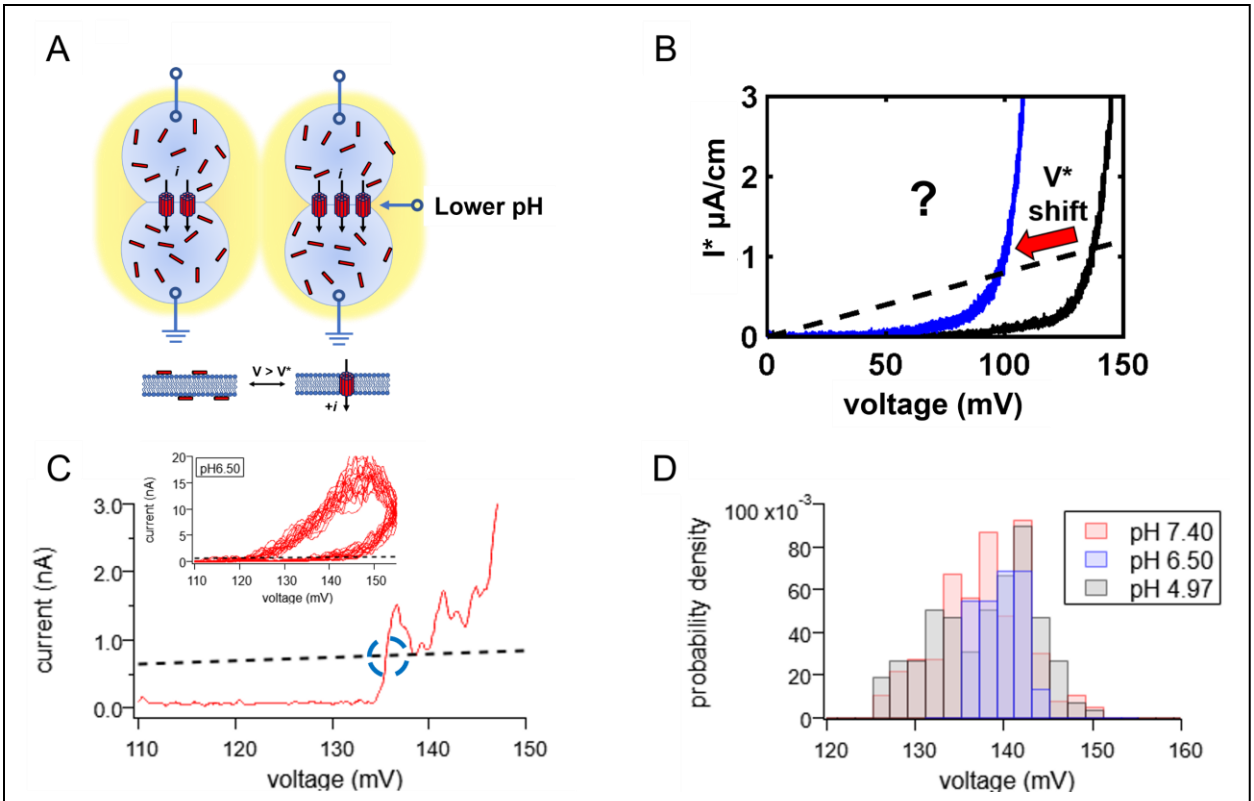

Figure 1. Process flow for characterizing shifts in V^* with changes in pH of droplet interface bilayers (DIBs) doped with alamethicin. **A.** Schematic for $V>V^*$ showing alamethicin undergoing a transition from monomers lying parallel to the bilayer surface (S-state) to their fully inserted state (I-state), where alm monomers oligomerize to form pores. **B.** Shifts in V^* are defined relative to shifts in the voltage, where the corresponding pore conductance exceeds the background conductance by one order of magnitude (dashed line, 8 µS/cm^2). **C.** Inset: Growth of the positive lobe of pinched hysteresis loops generated through cyclic voltammetry of alamethicin-DPhPC DIBs. Main: The first I/V pass through the hysteresis loop crosses the minimum detectable current threshold (dashed line) at V^* (highlighted with blue circle). **D.** Histograms of numerous V^* values at each of the three pH values studied, which were fitted to Gaussian distributions. The differences in the mean values for V^* were less (1-2 mV) than the widths (variances) of the distributions (4-9 mV), suggesting that any shifts in V^* were likely overwhelmed by the noise signal.

three different pH values (pH 4.97, 6.50, and 7.40). The three distributions were all well-fitted to Gaussian functions (SI), and aligned closely enough with each other that the differences of their mean values (1-2 mV) were much smaller than the variances (widths) of their distributions (4-9 mV). This suggests that noise levels were random and not correlated to changes in pH.

The number of monomers that form a channel in the lipid bilayer and the charge per monomer that crosses the membrane both affect the V^* threshold value. This is because alm-induced conduction is dependent on both voltage and peptide concentration [cite Hall and Vodyanoy alm review, *Biophys. J.* **45**, 233 (1984)]. The V^* probability density distributions shown in Figure 1D will most likely change with changes in peptide concentration, to the extent that the V^* distributions at the three different pH values may become resolvable given enough of a concentration difference. The peptide concentration was kept constant ([alm] = 1 µM), at a low enough level that only voltage was responsible for ion channel formation in the membrane. [cite]

For comparison, the peptide concentration threshold for alamethicin pore formation in the absence of voltage is about 20 μM. [cite Sarles, eTLE]

A better strategy for characterizing memristive behavior at constant peptide concentration is with the time-dependent dynamics of ionic currents in response to voltage pulses. At constant peptide concentration, the dynamic state equation for the number of open pores in the membrane, N_a, can be expressed as a first-order kinetic equation [7]

$$\frac{dN_a}{dt} = n - mN_a \,, \tag{1}$$

where n represents the rate of conductive pore formation and m the rate of pore decay. This equation can be solved to give an expression for N_a as a function of time:

$$N_a = \frac{n}{m}(1 - e^{-mt}) \,. \tag{2}$$

In this expression, both n and m, the rates for pore opening and pore closing respectively, are probabilities which are strongly dependent on voltage. The voltage dependencies of the rates are given by the following relations:

$$n = n_0 e^{V/V_n} \,, \;\; m = m_0 e^{V/V_m}, \tag{3}$$

where n_0 is the pore formation rate at 0 V, which for alm has been determined to be about 10^3 pores/sec•cm^2, and m_0 is the corresponding pore decay rate at 0 V, roughly 20 sec^{-1}. [cite Mead, *J. Membrane Biol*. **14**, 143 (1973)] V_n and V_m are the voltages required to increase the pore formation rate or pore decay rate e-fold. Together, they are responsible for the rapid increase in the number of open pores per unit area with applied voltage, without an explicit dependence on the peptide concentration:

$$N_a = \frac{n_0}{m_0} e^{V\left(\frac{1}{V_n} + \frac{1}{V_m}\right)} \,. \tag{4}$$

Figure 2 shows how pH modulates memristance in the membrane in response to square voltage pulses, each of 0.5 sec in duration and separated by 2.0 sec. For Figures 2A and C, at pH 7.40 and pH 4.97, the exciting voltage was 140 mV, while for 2B, at pH 6.50, it was 145 mV. This provided insight into the relative importance of pH versus voltage, as well as help identify any interaction between the two. Figure 2A, B and C each show the current and the "potentiation" time constant, τ_p, which is the time needed for the number of open pores in the membrane, N_a, to reach steady-state values.

Each current trace in Figure 2A, B and C was fitted to an equation for the current (shown as black dashed lines aligned with current traces) that included N_a, the time-dependent number of open pores per unit area in the membrane, and an additional term for electrowetting of the DIBs, which consisted of an increase in lipid bilayer area with voltage, driven entropically by the expulsion of oil between the droplets as a function of applied voltage. [cite] The voltage and time dependence of the currents can be described by [7]

$$i(V,t) = G_u N_a(V,t) A(V,t) V \,, \tag{5}$$

where G_u is the ensemble average conductance of a single alm pore, or 1.03 nS, [cite 2019 JOVE] N_a (V, t) is the voltage and time dependent number of open pores in the membrane per unit area, A

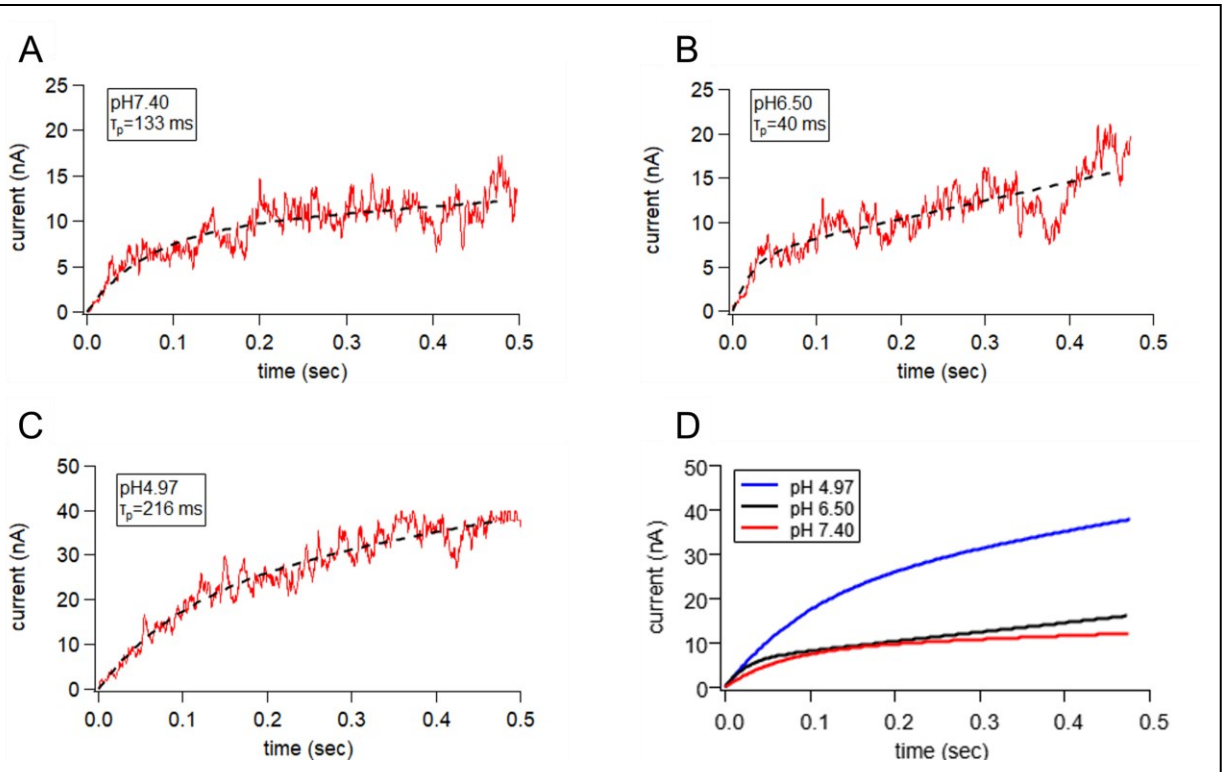

Figure 2. Changes in ionic currents from open alm pores in response to 500 msec width voltage pulses separated by 2000 msec, as a function of voltage and modulated by pH: **A.** pH 7.40, **B.** pH 6.50, **C.** pH 4.97. The stimulating voltage for 2A and 2C was 140 mV, and for 2B it was 145 mV. The red line segment on the y-axis of each plot is the highest current recorded at each pH value. The black dashed lines are fits of the currents using Equation (8). The two vertical dashed lines for each plot demarcate a "potentiation" time constant, τ_p, which is defined as the time needed for the number of open pores in the membrane to reach steady-state values. **D.** The fitted currents at the three pH values plotted for comparison. The current trace at pH 4.97 is clearly different from the other two pH values. Those at higher pH begin similarly but diverge at later times.

(V, t) is the bilayer area, and V is voltage. This expression can be resolved into contributions from N_a, given by Equation (2), and the membrane area, given by [cite Taylor 2015, 7]

$$A(V,t) = A_0\big(1 + A_m(V,t)\big)\,, \tag{6}$$

where A_0 is the membrane area at zero volts and A_m is the fractional increase in membrane area at an applied voltage:

$$A_m(V,t) = \frac{A(V,t) - A_0}{A_0}\,. \tag{7}$$

The dynamical response of A_m is given by

$$\frac{dA_m(V,t)}{dt} = \frac{1}{\tau_{ew}}\left(\alpha V^2 - A_m(V,t)\right)\,, \tag{8}$$

where τ_{ew} is a characteristic time constant for electrowetting (equals 1.5 sec for alamethicin-DPhPC bilayers at room temperature) and α is a steady-state gain coefficient [cite Taylor]. The final form for the fitted equation for current (Equation (5)) thus becomes

$$i(V,t) = G_u\left[\frac{n}{m}(1-e^{-mt})\right][1+bt]A_0V\ . \qquad (9)$$

By inspection, the term in the first set of brackets is Equation (2), and the second bracketed term fits the fractional change in area due to electrowetting at early times (at constant voltage, 50s-100s msec per pulse), when it is linear (compared to τ_{ew}=1.5 sec and later). In this case, $bt = A_m$, or equivalently, $b = \frac{A_m}{t}$. Both bracketed terms are integral to the memristance model described by Equation (5).

Figure 2D shows the current fits of Equation (9) at the three pH values from Figure 2A-C plotted together. Here, the combined effects of changing voltage and changing pH can be determined. The most noticeable difference occurs with pH 4.97 (Figure 2C), which has a significantly larger steady-state number of open pores (N_{as}) compared to the other two pH values. The "potentiation" times for reaching the steady-state numbers of open pores in the membrane, τ_p, were determined graphically from Equation (9) after removing the electrowetting term (SI). They are annotated in the text box for each of the three pH values shown in Figures 2A-C, and the corresponding fitted values for *n*, *m*, and *b* at each pH are listed in Table 1.

	Pore formation rate (pores/sec·cm²) (*n*)	Pore decay rate (1/sec) (*m*)	Steady-state N_{as} (pores/cm²) (*n*/*m*)	τ_p (msec)	$\frac{A_m}{t}$ (1/sec) (*b*)
pH 7.40 140 mV	$1.6{\cdot}10^6 \pm 4.4{\cdot}10^4$	15.6 ± 0.8	$1.0{\cdot}10^5$	133	0.8 ± 0.1
pH 6.50 145 mV	$2.0{\cdot}10^6 \pm 1.2{\cdot}10^5$	46.6 ± 3.3	$4.3{\cdot}10^4$	40	3.4 ± 0.1
pH 4.97 140 mV	$3.1{\cdot}10^6 \pm 4.8{\cdot}10^4$	11.0 ± 0.5	$2.7{\cdot}10^5$	216	1.4 ± 0.1

Table 1: Fitting parameters for the pulsed current (Equation (9), Figure 2D) at three pH values and two bias voltages. Includes alamethicin pore formation and decay rates, steady-state numbers of channels, potentiation times to reach steady-state currents, and membrane area increases due to electrowetting.

Discussion

Equation (9) is the fitting equation used to determine the variables responsible for the time-dependent dynamics of the pulsed currents in Figure 2. These parameters are *n*, *m*, and *b*, and are listed in Table 1, as functions of pH and bias voltage. Observations from the table that help deduce the connections between pH and memristive behavior include:

1. The pore formation rate (*n*) at pH 4.97 is significantly larger than at pH 6.50 or pH 7.40, which are closer together.
2. The pore decay rate (*m*) at pH 6.50 is significantly larger than at pH 4.97 or pH 7.40, which are closer together.
3. The steady state number of open pores (*n*/*m*) at pH 4.97 is significantly higher than at pH 6.50 or pH 7.40, which are closer together.
4. There is a much stronger electrowetting contribution to the pulsed currents (*b*) at pH 6.50 than at pH 4.97 or pH 7.40 because of the higher bias voltage used at pH 6.50 (145 mV vs. 140 mV).

5. The fitted currents at pH 7.40 (140 mV) and pH 6.50 (145 mV) are similar, but pH 6.50 has a much shorter potentiation time, τ_p, and higher average current levels than pH 7.40.

A reasonable starting point for a realistic membrane model with properties consistent with these observations is to combine the individual contributions to the dynamics from: (a) alamethicin pore formation and decay rates, and (b) time dependent electrowetting of DPhPC lipid bilayers. For (a), early studies characterizing the pore formation and decay dynamics of antimicrobial peptides like alamethicin in lipid bilayers have been primarily carried out with black lipid membranes (BLMs), which are single lipid bilayers "painted" across a hydrophobic aperture separating two aqueous compartments. Unlike DIBs, BLMs lack an oil phase, and hence do not have an electrowetting term like that in Equation (9). [cite Mead] In a BLM, the time course of the current response to voltage pulses has only two contributions. At early times, the first contribution is given by $\frac{n}{m}(1 - e^{-mt})$, which describes the time-dependent growth in the number of conductive open pores up to constant, steady state levels defined by $\frac{n}{m}$, the balanced ratio of pore formation to pore decay rates.

For case (b), because of electrowetting, the steady-state regime in DIBs is no longer a constant value but now increases linearly with time, under the influence of the second bracketed term in Equation (9), which is the change in the fractional membrane area. It is important to reiterate here that the linear time dependence for this term is an approximation which is accurate only for pulse widths significantly shorter than the τ_{ew} = 1.5 sec characteristic time constant for electrowetting with DPhPC lipid bilayers in hexadecane at room temperature. The total time dependence is given by Equation (6).

The values of the fitted parameters in Table 1 are consistent with models that focus on how surface charge affects pore formation of antimicrobial peptides (AMP) like alamethicin. [cite] Charge plays a major role in how biological membranes interact with molecules. For example, it has been shown that changes in the surface potential and surface charge density by proton titration of the ionizable groups in PS lipids result in changes to the elastic properties of the bilayer. [8,9] In the case of alamethicinm-DPhPC bilayers, two titrations of exchangeable hydrogens can occur as a function of pH, titration of the membrane surface charge, and titration of the alamethicin channel conductance. Changes to the surface charge of the lipids strongly affect the hydrophobic matching of the peptide pore with the bilayer, a critical parameter for peptide insertion and pore formation in the membrane.[10] Moreover, hydrophobic mismatches resulting from charge cause the system to move away from conformational equilibrium by inducing high lateral pressures on alamethicin, the result of headgroup electrostatic repulsion and reduced conformational entropy within the hydrophobic core of the membrane. [11] For a well-ordered bilayer, this pressure is usually balanced by a negative lateral tension at the aqueous interface. However, this balance can be easily disrupted by nucleation of defects resulting from the distortion of membrane lipids surrounding the ion channel.

Zwitterionic lipids, such as DPhPC, are also affected by added charge, but in different ways than net charged lipids. For example, at pH 7.40, there are more OH^- ions than H^+ ions in solution. Also, since OH^- ions are polarizable, while H^+ ions are not, we expect OH^- to associate more with the

PC headgroups, resulting in a net negatively charged membrane. [12] The isoelectric points of PC lipids (determined from electrophoretic mobility measurements of vesicles) occur at around pH=4. In terms of acid-titratable groups on DPhPC, the pKa of both the phosphate (pKa ~1) and choline (pKa~11) groups are out of bounds. However, the pKa of alamethicin's negatively charged carboxylate groups on glutamate residues that line the lumen of the alamethicin pore is reported to be pKa~5.3-5.7, not unlike those of other antimicrobial membrane peptides. [13-16] This is well within the range of pH values studied here (pH 7.40, pH 6.50, pH 4.97).[17] At pH 4.97, these charged groups are neutralized, which stabilizes pore formation and the number of open pores in the bilayer by screening the electrostatic repulsion of α-helix dipoles. [Boheim, 1974] The other two pH values are both above the pK_a value of the peptide but were maintained at different voltages from each other (the pulses at pH 6.50 were kept at 145 mV, while the other two pH values were pulsed at 140 mV). This affects both the number of pores per unit area and the membrane area itself, but in different ways than by changing pH at constant voltage.

The accepted model for pore formation with alamethicin involves a rotation and oligomerization of peptide monomers in the membrane. [18,19] Alamethicin's large dipole moment (70-80 D) plays an important role in its voltage-dependent gating mechanism. Upon application of a voltage greater than V^*, the interaction of the dipole with the electric field causes alamethicin monomers to rotate and insert into the membrane, aligning with the lipid fatty acid tails. Once inserted, peptide monomers can diffuse within the membrane, eventually forming oligomeric conductive pores. The peptide's negatively charged glutamate residues at neutral pH near its C-terminus are thought to help anchor it in the membrane through a network of hydrogen bonds with water and the lipid headgroups, allowing the positively charged N-terminus to traverse the membrane during insertion. However, changing the pH causes H^+ and OH^- ions to migrate into the membrane, thus changing both the surface charge and the electric field in the alamethicin pore. [20]

The increase in pore activity that we observed at lower pH values is consistent with reports of enhanced probability for alamethicin pore formation. [8] While increased acidity enhanced the probability of a pore being in a higher conductance state, the channel conductance itself was largely unaffected. [8] This is an important observation, since it shows that the enhanced currents at lower pH are due simply to increases in the numbers of active channels in the membrane, and not intrinsic pore conductance.

For alamethicin, aggregation of peptide monomers to form pores reduces energetically costly peptide-lipid interactions due to hydrophobic mismatch. In this case, transitions between different conductance states correspond to the reversible addition of monomers to an existing pore as a function of voltage. As the concentration of peptide monomers increases, positive cooperativity for attraction to the lipids in the membrane emerges due to oligomerization. Aggregates cannot dissociate from the membrane as easily as monomers can, providing a thermodynamic driving force for pore formation. [Mead, 1973] Higher conductance states correspond to larger oligomers. This results in a distribution of pore sizes in the membrane that corresponds to the distribution of conductance levels.

Partitioning of membrane peptide monomers from the aqueous phase to the membrane phase is largely driven by the hydrophobicity of the peptide. The overall hydrophobicity is related to the

amino acids that make up the peptide of interest, as it is well known that alamethicin's 20 different amino acids themselves have largely different partitioning behaviors between polar and nonpolar environments. [30] Additionally, the naturally charged amino acids have variable hydrophobicity values that are dependent on their charge state. Looking specifically at glutamate, the free energy of transfer ΔG of this residue from water to a POPC bilayer decreases from 2.02 in the negatively charged state to -0.01 in the neutral protonated state, leading to a favorable transfer of peptide from water to the surface of a POPC bilayer.[30] Here, we observe that pore formation rates, pore decay rates, and steady-state numbers of active channels all increase as a function of decreasing pH below the pKa of the two glutamate residues in alamethicin (~5.3-5.7). This can be rationalized by an increase in alamethicin hydrophobicity, and consequently, increased alamethicin monomer partitioning to the membrane from the aqueous phase. With more alamethicin monomers on the membrane surface at pH 4.97 compared to 7.40, passing the voltage threshold for insertion leads to a greater number of pores that are formed faster and that are stable for longer times. This is not dissimilar to the membrane association and insertion process of the pH-low insertion peptide (pHLIP), where changes in peptide hydrophobicity increases due to pronation of charged amino acid residues, culminating in membrane insertion. [31]

Conclusions

We found that decreasing pH below the pKa of the glutamate residues of alamethicin resulted in increased current levels, due to increased partitioning of alamethicin monomers in the membrane, and stabilization of the pore lumen of the oligomers by screening the electrostatic repulsion of α-helix dipoles. Lowering pH also resulted in the neutralization of the initially negatively charged DPhPC bilayer, which amplified hydrophobic mismatch by locally increasing membrane curvature stress at the pore. Larger oligomers were thermodynamically stabilized relative to monomers by this stress, resulting in an additional driving force for oligomerization. This is an example of how collective motions in the membrane impart "force from lipid" effects on biomembrane molecules.[32] These local forces can modulate mechanisms of protein function and are seen most often in mechanosensitive ion channels, but have been observed in many other contexts, including alamethicin pore formation described here. Changing pH changes the ionic currents from alamethicin pores in a similar manner as changing the voltage would, [33] except for the fact that here it's an indirect effect that can extend over many synapses and neurons within the context of heterosynaptic plasticity.

Recently we reported a downward shift in the V^* threshold voltages for alamethicin pore formation as a function of aqueous macromolecular crowding in the droplets of a DIB, but in that case, it was due to increased chemical activity of alamethicin peptides in solution and increased osmotic stress in the bilayers due to the excluded volumes in the pores that were inaccessible to the polymers.[34] These changes resulted in a large enough effective concentration increase in peptide monomers at the membrane to change V^*, which is not the case here. Instead, the distributions of V^* values did not seem to change with changes in pH beyond random error. The chemical potentials of the peptide monomers at the solution concentrations of alamethicin used here (1 μM) were apparently not high enough to result in clear changes in V^*, which depends on concentration. However, the kinetics for pore formation in pulsed experiments did change with pH in predictable ways that could be easily rationalized.

Thresholds are ubiquitous in neuromorphic networks, starting with the earliest networks known as perceptrons, which featured thresholds as the defining computational element.[35] Many biological systems use time differences between action potentials ('spikes') to encode information, which has led to the development of artificial networks of 'spiking neurons' as the computational elements. Also known as 'integrate-and-fire neurons', these model systems rely on thresholds in both voltage, current, and time (i.e., refractory periods) for computation. Soft-matter neuromorphic devices like the biomolecular memristors described here can be configured as spiking neural networks (SNNs), which are ideally suited for processing temporal data at a fraction of the energetic cost and number of resources (synapses, neurons) needed in traditional convolution-based neuromorphic networks.[36] Heterosynaptic plasticity in bioinspired SNNs, enabled by tuning environmental variables like pH, can provide additional programmable elements that will make these models more biologically realistic, and enhance both their functionality and flexibility for AI and machine learning applications.

Materials and Methods

Materials Potassium chloride (KCl), 3-(*N*-morpholino)propanesulfonic acid (MOPS) buffer, sodium acetate (NaAc) buffer, sodium hydroxide, agarose powder (p/n A9539), and ethanol were obtained from Sigma-Aldrich. Alamethicin was dissolved in ethanol to a concentration of 5 mg/mL to create a stock solution used for further sample preparation, and the stock solution was stored at −20 °C when not in use. Liposome solutions were prepared by dissolving 1,2-diphytanoyl-*sn*-glycero-3-phosphocholine (DPhPC) lipids (Avanti, Alabaster, AL) at 2 mg/mL in buffer (10 mM MOPS or 100 mM NaAc, 500mM KCl, NaOH to obtain pH 7.45 with MOPS or pH 5 with NaAc) and extruding the resulting multilamellar vesicles 51 times through a miniextruder (Avanti) containing a track-etched 100 nm polycarbonate membrane creating large unilamellar vesicles (LUVs).

Assembly Synaptic mimic assembly was based on the droplet interface bilayer (DIB) method, which has been used extensively in recent years to study the biophysics of bioarchitectural memristive systems.[7] Concentrations for peptides were assigned using the molar ratio of available lipid to peptide and were L/P = 788 (3μM alamethicin). Peptides were suspended in aqueous buffer at 500mM KCl and 2.4 mM DPhPC (as 100 nm extruded vesicles) unless mentioned otherwise. Aqueous droplets of 500nL volume were manually pipetted to agarose-coated silver/silver-chloride electrodes. Data was recorded using a patch clamp amplifier (Axopatch 1D, Molecular Devices, San Jose, CA). Capacitive current response to 10Hz, 10mV triangular voltage sweeps (Agilent) was used to monitor bilayer formation and thickness.[37] Bright field images were acquired using the 4x objective of an inverted Nikon TE-300 optical microscope.

Recording and Analysis Alamethicin activity was assessed in response to a cyclic triangular voltage waveform, using bipolar cyclic voltammetry (CV) scans. Scan rates were run at 100, 250, and 500 mV/s (Stanford Research Systems D345). Amplitudes were chosen to elicit current responses greater than 1 nA. Alamethicin was added in equal amounts to both sides of the membrane. Aqueous buffer and electrolyte were also identically added to each side of the DIB. Quantitatively, conductive pore formation was achieved once the specific membrane conductance

in the presence of alamethicin increased beyond a threshold of G^*= 8μS/cm^2 (Figure 1B), which we estimate to be about an order of magnitude greater than the background conductance of a DPhPC lipid bilayer without the presence of alm. The voltage that gives rise to the specific current that crosses the 8μS/cm^2 line is the threshold voltage, V^*, that must be exceeded to create a conductive pore. The conductance can then be expressed as $G = i/(V-V^*)$, which requires $V > V^*$ for the onset of nonzero currents.[31]

Current/voltage (I/V) plots were generated from the averages of five consecutive time-dependent segments taken from bipolar CV scans of DPhPC lipid bilayers with alm channels at three different scan rates, 100, 250, and 500 mV/s, after removing the capacitive currents.[38] Histograms of V^* values for the rising and falling segments at each scan rate were generated with a script written in Igor Pro programming language (Wavemetrics) from numerous (ca. 100) I/V curves and converted to probability density distributions by normalizing the total areas under the curves to one.

Conflict of interest statement
On behalf of all authors, the corresponding author states that there is no conflict of interest.

Data availability
The datasets generated during and/or analysed during the current study are available from the corresponding author on reasonable request.

ORCID
W.T. McClintic, 0000-0003-3234-0053
F. Barrera, 0000-0002-5200-7891
C.D. Schuman, 0000-0002-4264-8097
C.P. Collier, 0000-0002-8198-793X

Acknowledgements
This work was supported by National Institutes of Health grant R35GM140846 (to F.N.B.). DB is supported through the National Science Foundation, Division of Molecular and Cellular Biosciences(MCB), under contract no. 2219289. W.M. acknowledges support from the Bredesen Center for Interdisciplinary Research. Preparation of peptidoliposomes for bilayer formation was carried out at the Department of Biochemistry & Cellular and Molecular Biology, University of Tennessee, Knoxville. Electrophysiological measurements on droplet interface bilayers were conducted at the Center for Environmental Biotechnology, University of Tennessee, Knoxville, and at the Center for Nanophase Materials Sciences, which is a DOE Office of Science User Facility. We thank Dr. Larry Millet at the Center for Environmental Biotechnology for the generous use of laboratory space. Notice: This manuscript has been authored by UT-Battelle, LLC, under Contract No. DE-AC0500OR22725 (to C.D.S.) with the U.S. Department of Energy. The United States Government retains and the publisher, by accepting the article for publication, acknowledges that the United States Government retains a nonexclusive, paid-up, irrevocable, worldwide license to publish or reproduce the published form of this manuscript, or allow others to do so, for the United States Government purposes.

Note: The authors have no conflicts of interest to declare.

References

1. Bailey, C.H., Giustetto, M., Huang, Y.Y., Hawkins, R.D., Kandel, E.R. "Is Heterosynaptic Modulation Essential for Stabilizing Hebbian Plasticity and Memory?", *Nat. Rev. Neurosci.***1**, 11-20 (2000).
2. Purves, D., Augustine, G.J., Fitzpatrick, D., Hall, W.C., LaMantia, A.S., White, L.E. "Synaptic Plasticity." In: *Neuroscience* (5th ed.) (pp. 163-182). Sunderland, Massachusetts: Sinauer Associates.
3. Long, T.Y., Zhu, L.Q., Ren, Z.Y., Guo, Y.B., "Global Modulatory Heterosynaptic Mechanisms in Bio-polymer Electrolyte Gated Oxide Neuron Transistors", *J. Phys. D Appl. Phys.* 435105 (2020).
4. Yang, Y., Chen, B., Lu, W.D., "Memrisitive Physically Evolving Networks Enabling Emulation of Heterosynaptic Plasticity", *Adv. Mater.* **27**, 7720-7727 (2015).
5. Patelska, A.D., Figaszewski, Z.A., "Effect of pH on the Interfacial Tension of Lipid Bilayer Membranes", *Biophys. J.* **78**, 812-817 (2000).
6. Andersson, M., Jackman, J., Wilson, D., Jarvoll, P., Alfredsson, V.; Okeyo, G., Duran, R., "Vesicle and Bilayer Formation of Diphytanoylphosphatidylcholine (Dphpc) and Diphytanoylphosphatidylethanolamine (Dphpe) Mixtures and their Bilayers' Electrical Stability", *Colloids Surf., B* **82**, 550-561 (2011).
7. Najem, J.S., Taylor, G.J., Weiss, R.J., Hasan, M.S., Rose, G., Schuman, C.D., Belianinov, A., Collier, C.P., Sarles, S.A., "Memristive Ion Channel-Doped Biomembranes as Synaptic Mimics", *ACS Nano* **12**, 4702-4711 (2018).
8. Bezrukov, S.M., Rand, R.P., Vodyanoy, I., Parsegian, V.A., "Lipid Packing Stress and Polypeptide Aggregation: Alamethicin Channel Probed by Proton Titration of Lipid Charge", *Faraday Discuss.* **111**, 173-183 (1998).
9. Bezrukov, S.M., "Functional Consequences of Lipid Packing Stress", *Curr. Opin. Colloid Interface Sci.***5**, 237-243 (2000).
10. Killian, J.A., "Hydrophobic Mismatch between Proteins and Lipids in Membranes", *Biochim. Biophys. Acta* **1376**, 401-416 (1998).
11. Cantor, R.S., "The Influence of Membrane Lateral Pressures on Simple Geometric Models of Protein Conformational Equilibrium", *Chem. Phys. Lipids* **101**, 45-56 (1999).
12. Zhou, Y., Raphael, R.M., "Solution pH Alters Mechanical and Electrical Properties of Phosphotidylcholine Membranes: Relation between Interfacial Electrostatics, Intramembrane Potential, and Bending Elasticity", *Biophys. J.* **92**, 2451-2462 (2007).
13. Hanz, S.Z., Shu, N.S., Qian, J., Christman, N., Kranz, P., An, M., Grewer, C., Qiang, W., "Protonation-Driven Membrane Insertion of a pH-Low Insertion Peptide", *Angew. Chem. Int. Ed.* **55**, 12376-12381 (2016).
14. Alves, D.S., Westerfield, J.M, Shi, X., Nguyen, V.P.; Stefanski, K.M., Booth, K.R., Kim, S., Morell-Falvey, J., Wang, B.C., Abel, S.M., Smith, A.W., Barrera, F.N., "A Novel pH-Dependent Membrane Peptide that Binds to EphA2 and Inhibits Cell Migration", *eLife* **7**, e36645 (2018).
15. Scott, H.L., Westerfield, J.M., Barrera, F.N., "Determination of the Membrane Translocation pK of the pH-Low Insertion Peptide", *Biophys. J.* **113**, 869-879 (2017).

16. Scott, H.L., Nguyen, V.P., Alves, D.S., Davis, F.L., Booth, K.R., Bryner, J., Barrera, F.N., "The Negative Charge of the Membrane has Opposite Effects on the Membrane Entry and Exit of pH-Low Insertion Peptide", *Biochem.* **54**, 1709-1712 (2015).
17. Chiriac, R., Luchian, T., "pH Modulation of Transport Properties of Alamethicin Oligomers Inserted in Zwitterionic-Based Artificial Membranes", *Biophys. Chem.* **130**, 139-147 (2007).
18. Huang, H.W., Wu, Y., "Lipid-alamethicin Interactions Influence Alamethicin Orientation", *Biophys. J.* **60**, 1079-1087 (1991).
19. He, K., Ludtke, S.J., Heller, W.T., Huang, H.W., "Mechanism of Alamethicin Insertion in Lipid Bilayers", *Biophys. J.* **71**, 2669-2679 (1996).
20. Hall, J.E., Vodyanoy, I., Balasubramanian, T.M., Marshall, G.R., "Alamethicin, A Rich Model for Channel Behavior", *Biophys. J.* **45**, 233-247 (1984).
21. Keller, S.L., Mezrukov, S.M., Gruner, S.M., Tate, M.W., Vodyanoy, I., Paresgian, V.A., "Probability of Alamethicin Conducting States Varies with Nonlamellar Tendency of Bilayer Phospholipids", *Biophys. J.* **65**, 23-27 (1993).
22. Cantor, R.S., "Size Distribution of Barrel-Stave Aggregates of Membrane Peptides: Influence of the Bilayer Lateral Pressure Profile", *Biophys. J.* **82**, 2520-2525 (2002).
23. Fox Jr., R.O., Richards, F.M., "A Voltage-Gated Ion Channel Model Inferred from the Crystal Structure of Alamethicin at l.5-Å Resolution", *Nature* **300**, 325-330 (1982).
24. Nagao, T., Mishima, D., Javkhlantugs, M., Wang, J., Ishioka, D., Yokota, K., Norisada, K., Kawamura, I., Ueda, K., Naito, A., "Structure and Orientation of Antibiotic Peptide Alamethicin in Phospholipid Bilayers as Revealed by Chemical Shift Oscillation Analysis of Solid State Nuclear Magnetic Resonance and Molecular Dynamics Simulation", *Biochim. Biophys. Acta Biomembr.* **1848**, 2789-2798 (2015).
25. Gruner, S.M., "Stability of Lyotropic Phases with Curved Interfaces", *J. Phys. Chem.* **93**, 7562-7570 (1989).
26. Ben-Shaul, A., 1995. "Molecular Theory of Chain Packing, Elasticity and Lipid–Protein Interaction in Lipid Bilayers". In: *Dynamics of Membranes*. Elsevier: North Holland, Amsterdam, pp. 359–401.
27. Seddon, J.M., Templer, R.H., 1995. "Polymorphism of Lipid-Water Systems". In: Lipowsky, R., Sackmann, E. (Eds.), *Structure and Dynamics of Membranes*. Elsevier: North Holland, Amsterdam, pp. 97–160.
28. Helfrich, W. 1981. "Amphiphilic Mesophases Made of Defects". In: *Physics of Defects*. R. Balian, M. Kle´man, and J.-P. Poirier, editors. North Holland, Amsterdam, The Netherlands. 716–755.
29. Marsh, D., "Lateral Pressure Profile, Spontaneous Curvature Frustration, and the Incorporation and Conformation of Proteins in Membranes". *Biophys. J.* **93**, 3884-3899 (2007).
30. Hasan, M.S., Schuman, C.D., Najem, J.S., Weiss, R., Skuda, N.D., Belianinov, A., Collier, C.P., Sarles, S.A., Rose, G.S., "Biomimetic, Soft-Material Synapse for Neuromorphic Computing: from Device to Network", 2018 IEEE 13th Dallas Circuits and Systems Conference (DCAS).
31. Eisenberg, M., Hall, J.E., Mead, C.A., "The Nature of the Voltage-Dependent Conductance Induced by Alamethicin in Black Lipid Membranes", *J. Membrane Biol.* **14**, 143-176 (1973).
32. Anishkin, A., Loukin, S.H., Teng, J., Kung, C., "Feeling the Hidden Mechanical Forces in Lipid Bilayer is an Original Sense", *Proc. Natl. Acad. Sci., U.S.A.* **111**, 7898-7905 (2014).

33. Opsahl, L.R., Webb, W.W., “Transduction of Membrane Tension by the Ion Channel Alamethicin”, *Biophys. J.*, **66**, 71-74 (1994).
34. McClintic, W.T., Taylor, G.J., Simpson, M.L., Collier, C.P., “Macromolecular Crowding Affects Voltage-Dependent Alamethicin Pore Formation in Lipid Bilayer Membranes”, *J. Phys. Chem. B* **124**, 5095-5102 (2020).
35. Maass, W., “Networks of Spiking Neurons: The Third Generation of Neural Network Models”, *Neural Networks* **10**, 1659-1671 (1997).
36. Schuman, C.D., Potok, T.E., Young, S., Patton, R., Perdue, G., Chakma, G., Wyer, A., Rose, G.S., “Neuromorphic Computing for Temporal Scientific Data Classification”, in *Proceedings of the Neuromorphic Computing Symposium*. 2017, Knoxville, TN.
37. Taylor, G.J., Venkatesan, G.A., Collier, C.P., Sarles, S.A., “Direct *in situ* Measurement of Specific Capacitance, Monolayer Tension, and Bilayer Tension in a Droplet Interface Bilayer”, *Soft Matter* **11**, 7592-7605 (2015).
38. Okazaki, T., Sakoh, M., Nagaoka, Y., Asami, K., “Ion Channels of Alamethicin Dimer N-Terminally Linked by Disulfide Bond”, *Biophys. J.* **85**, 267-273 (2003).